

Microphase Separation Transition and Rheology of Side-Chain Liquid-Crystalline Block Copolymers

Kyung Min Lee and Chang Dae Han*

Department of Polymer Engineering, The University of Akron, Akron, Ohio 44325

Received November 20, 2001; Revised Manuscript Received January 31, 2002

ABSTRACT: Microphase separation was induced from *homogeneous* polystyrene-*block*-polyisoprene (SI diblock) copolymer by grafting of a liquid-crystalline (LC) monomer onto the polyisoprene (PI) block. The origin of the formation of microdomain structure in the side-chain LC block copolymer from a *homogeneous* SI diblock copolymer is explained in terms of a dramatic increase in repulsive segmental interactions between the constituent blocks. For the investigation, three homogeneous SI diblock copolymers with varying block length ratios (SI-5/6, SI-10/6, and SI-14/3) were synthesized via anionic polymerization in tetrahydrofuran as solvent. This resulted in PI blocks having the following microstructures: 34% 1,2-addition, 59% 3,4-addition, and 7% 1,4-addition. Subsequently, the PI blocks in each of the SI diblock copolymers were first hydroxylated via hydroboration/oxidation reactions to yield hydroxylated SI diblock copolymers (SI-5/6-OH, SI-10/6-OH, and SI-14/3-OH), and then a liquid-crystalline (LC) monomer, 6-[(4-cyano-4'-biphenyl)oxy]hexanoic acid (5CN-COOH), synthesized in our laboratory, was grafted onto the hydroxylated PI blocks (PI-OH), yielding side-chain LC diblock copolymers (SI-5/6-5CN, SI-10/6-5CN, and SI-14/3-5CN). The disappearance of the -COOH and -OH groups after coupling reaction was confirmed using ^1H nuclear magnetic resonance spectroscopy and infrared spectroscopy. Transmission electron microscopy revealed that at room temperature SI-5/6-5CN has spherical microdomains, SI-10/6-5CN has hexagonally packed cylindrical microdomains, and SI-14/3-5CN has lamellar microdomains. The LC phase of the side-chain block copolymers was identified using polarizing optical microscopy. The clearing temperature (T_{cl}), determined by differential scanning calorimetry, of the side-chain LC block copolymers is found to be ca. 84 °C, whereas the T_{cl} of LC monomer 5CN-COOH is 170 °C. Oscillatory shear rheometry indicates that the sphere-forming block copolymer SI-5/6-5CN undergoes a lattice disordering/ordering transition at 140 °C and a demicellization/micellization transition at 155 °C, while both the cylinder-forming block copolymer SI-10/6-5CN and lamella-forming block copolymer SI-14/3-5CN undergo microphase separation transition at temperatures much higher than 240 °C, the highest experimental temperature employed. Binodal curves exhibiting upper critical solution temperature were constructed, via cloud point measurement, for four pairs of polystyrene (PS) and PI grafted with 5CN-COOH (PI-5CN). An expression for the temperature dependence of the Flory-Huggins interaction parameter χ for the PS/(PI-5CN) pair was determined and compared with the χ expression for the PS/PI pair. The origin of the formation of microdomain structure in the side-chain LC block copolymers SI-5CN from a *homogeneous* SI diblock copolymer is explained in terms of molecular weight, block composition, and χ for the PS/(PI-5CN) pair.

Introduction

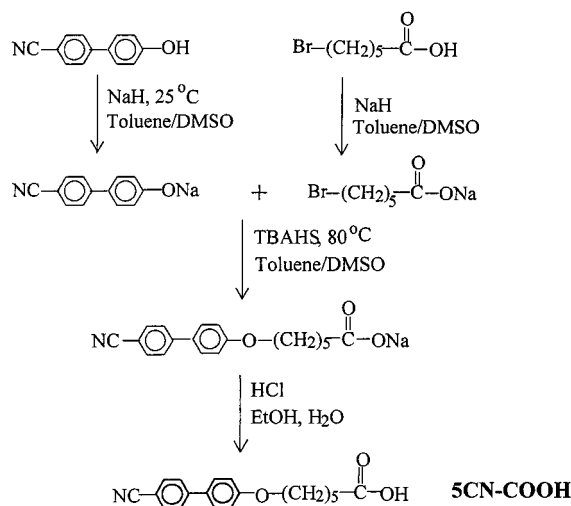
During the past decade, a number of research groups^{1–26} have synthesized liquid-crystalline (LC) block copolymers and investigated their morphology and phase behavior. Basically, there are two types of LC block copolymer: main-chain LC block copolymer, in which one of the blocks consists of rigid chains exhibiting liquid crystallinity, and side-chain LC block copolymer, in which mesogenic groups are grafted onto one of the block-forming side chains. The unique feature of LC block copolymer lies in that, upon heating, it may undergo both microphase separation transition (MST) or order-disorder transition (ODT) due to the presence of microdomains and isotropization owing to the presence of the LC phase. Thus, with a judicious choice of molecular weight, composition of the constituent blocks, and the chemical structure of the LC phase, it is possible, in principle, to control the MST temperature (T_{MST}) or ODT temperature (T_{ODT}) of the separated microphase and the clearing temperature (T_{cl}) of the LC phase independently.

To facilitate our discussion later in this paper, let us consider side-chain LC AB-type diblock copolymers that are synthesized by grafting LC monomer onto one of the diblocks. In general, the molecular weight of LC mono-

mer is on the order of hundreds. Thus, after an LC monomer is grafted onto one of the blocks, the molecular weight of the resulting side-chain LC block copolymer will become very high. It should be pointed out that under such a situation not only are the molecular weight and block composition altered after the LC monomer is grafted onto an AB-type diblock copolymer, but also the segmental interactions between the constituent block components. It has been found that measurement of T_{MST} or T_{ODT} often becomes practically impossible, *unless* the molecular weight of the starting block copolymer is very low. These considerations were what prompted us to launch a research project, the results of which are presented in this paper.

The organization of this paper is as follows. First we present the synthesis and characterization of three *homogeneous* low-molecular-weight polystyrene-*block*-polyisoprene (SI diblock) copolymers having varying block length ratios and an LC monomer, 6-[(4-cyano-4'-biphenyl)oxy]hexanoic acid (5CN-COOH). We also describe modifications of the SI diblock copolymers first by hydroboration/oxidation of the polyisoprene (PI) block of the SI diblock copolymer, yielding hydroxylated SI diblock copolymer (SI-OH), and then by grafting of 5CN-COOH onto the hydroxylated PI block (PI-OH), yielding

Scheme 1

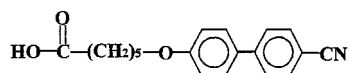


side-chain LC diblock copolymer (SI-5CN). We show thermal transitions in the LC phase of SI-5CN as determined by differential scanning calorimetry and phase transitions in the microphase-separated block copolymer, SI-5CN, as determined by oscillatory shear rheometry. We present the type of LC phase in the SI-5CNs as revealed by polarizing optical microscopy and the microdomain structures of the SI-5CNs as characterized by transmission electron microscopy. We discuss segmental interactions for a pair of polystyrene (PS) and PI grafted with 5CN-COOH (PI-5CN), incorporating the phase diagram constructed from cloud point measurements. On the basis of the information for the segmental interactions between PS and PI-5CN, we explain the origin of the formation of microdomains in the side-chain LC diblock copolymer SI-5CN after an LC monomer 5CN-COOH is grafted onto the PI block of a *homogeneous* SI diblock copolymer.

Experimental Section

Synthesis of Polymers. Three homogeneous SI diblock copolymers with varying block length ratios (SI-5/6, SI-10/6, and SI-14/3) were first synthesized via anionic polymerization in tetrahydrofuran (THF) as solvent. This resulted in PI blocks having the following microstructures: 34% 1,2-addition, 59% 3,4-addition, and 7% 1,4-addition. Subsequently, the PI blocks in each of the SI diblock copolymers were hydroxylated via hydroboration/oxidation reactions to yield hydroxylated SI diblock copolymers (SI-5/6-OH, SI-10/6-OH, and SI-14/3-OH). The readers are referred to our previous paper for the details of the synthesis of the SI-OH.²⁷ Also, we synthesized, via anionic polymerization, three polyisoprenes with varying molecular weights (PI-4, PI-13, and PI-100) using the standard procedures, and subsequently they were hydroxylated, via hydroboration/oxidation reactions, to obtain hydroxylated polyisoprene (PI-OH).

In this study, we synthesized a liquid-crystalline monomer 6-[(4-cyano-4'-biphenyl)oxy]hexanoic acid with the chemical structure



Hereafter this chemical structure will be referred to as 5CN-COOH. The reaction route for the synthesis of 5CN-COOH is shown in Scheme 1. Briefly stated, 1 mol of 4-cyano-4'-hydroxybiphenyl and 1.1 mol of sodium hydride were dissolved into a three-neck flask with 12 mL of mixed solvent consisting of toluene and dimethyl sulfoxide (DMSO) (5:1 v/v).

The mixture was stirred for 4 h at room temperature, and then the temperature was increased to 60 °C and kept there for 1 h before use. Tetrabutylammonium hydrogen sulfate (TBAHS) was added to the 6-bromohexanoic acid solution, while stirring for 30 min at 60 °C, which then was added dropwise into a three-neck flask containing 4-cyano-4'-hydroxybiphenyl solution. The mixture was then heated to 80 °C, at which the reaction continued for 24 h. The solution was cooled to room temperature and then poured into a mixture consisting of 3 M hydrochloric acid (HCl) and water, whereby the reaction product was strongly acidified with HCl solution. After the crude product was precipitated, it was filtered and washed three times with water. The solid obtained was washed three times with a mixed solvent consisting of ethanol and water (1:4 v/v) to remove unreacted 4-cyano-4'-hydroxybiphenyl, filtered, and then dried in a vacuum oven at 50 °C for 1 day. Finally, the crude product was recrystallized from methanol and then dried in a vacuum oven at 50 °C for 2 days. The liquid crystal monomer was chlorinated using thionyl chloride before being reacted with an SI-OH diblock copolymer. To protect the active group in the acid chloride before being reacted with an SI-OH, the chlorinated monomer was first dissolved in anhydrous THF.

The grafting of LC monomer 5CN-COOH onto the PI-OH block of SI-OH was accomplished by following the reaction route, as shown in Scheme 2. Briefly stated, a predetermined amount of SI-OH (1 mol of OH), which was just dried in a vacuum oven at 40 °C, was dissolved in 10 mL mixture of anhydrous THF and pyridine (1:1 v/v) in a three-necked flask with stirrer at room temperature under argon gas. After stirring for 1 h, 1.2 mol of chlorinated 5CN-COOH solution in anhydrous THF was added dropwise into the reaction flask for 30 min at 0 °C; the reaction temperature was increased gradually to room temperature and maintained there for 24 h. The reaction mixture was poured into ethanol/water (1:1 v/v), and the crude product was precipitated, which was then filtered and washed several times with ethanol/water (1:1 v/v). The polymer was extracted with methanol using a Soxhlet extractor for 24 h. Subsequently, the final product, SI-5CN, was dried in a vacuum oven at 30 °C for 2 days and at 60 °C for 1 day.

Also, 5CN-COOH was grafted onto three PI-OHs to obtain PI-5CNs. For cloud point measurements, varying amounts of 5CN-COOH were grafted to PI-4-OH, such that 5, 50, 80, or 100% of hydroxyl groups in PI-4-OH could be reacted with 5CN-COOH. In this study, PI-4-5CN polymers with varying amounts of 5CN-COOH were used to prepare binary blends with homopolymer polystyrene (PS) for cloud point measurements.

Structure Characterization. The chemical structures of the polymers synthesized (SI-5CN and PI-5CN) were characterized using nuclear magnetic resonance (NMR) spectroscopy and Fourier transform infrared (FTIR) spectroscopy. For such purposes, both ¹³C and ¹H NMR spectra were obtained using a spectrometer (Varian Gemini-200, 200 MHz). Films suitable for FTIR were prepared by casting 2% (w/v) solution in THF or chloroform directly on the KBr salt plate. Film thickness was adjusted, such that the maximum absorbance of any band was less than 1.0, at which the Beer-Lambert law is valid. FTIR spectra were obtained using a Perkin-Elmer spectrometer (model 16PC FTIR). Spectral resolution was maintained at 4 cm⁻¹.

Molecular Weight Determination. The number-average molecular weights (*M_n*) of three SI diblock copolymers synthesized (SI-5/6, SI-10/6, and SI-14/3) were determined using vapor pressure osmometry (Knauer) and also membrane osmometry (Jupiter Instrument). The *M_n* of PI-4 was determined using vapor pressure osmometry (Knauer), and the *M_n*'s of PI-13 and PI-100 were also determined using membrane osmometry (Jupiter Instrument). The polydispersity (*M_w*/*M_n*) of all the polymers synthesized was determined using gel permeation chromatography (GPC, Waters). The results are summarized in Table 1. Also given in Table 1 is the weight fraction of polystyrene in each SI diblock copolymer, which was determined using ¹H NMR spectroscopy. We found that an

Scheme 2

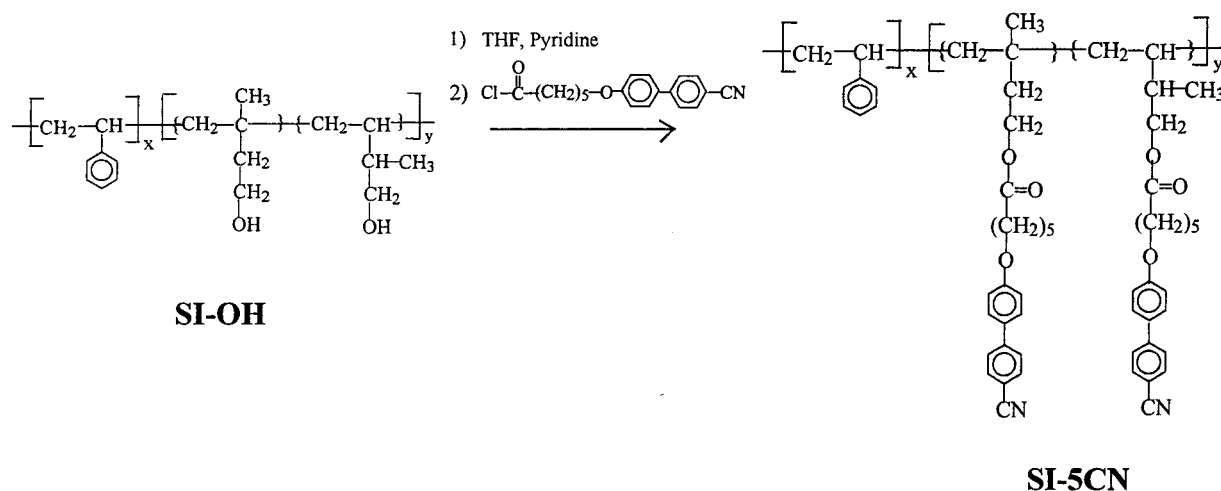


Table 1. Molecular Characteristics of the SI and SI-5CN Diblock Copolymers Synthesized in This Study

sample code	M_n (g/mol) ^a	M_n (g/mol) ^b	M_w/M_n ^c	PS (wt frac) ^d	morphology
SI-5/6	1.03×10^4 ^a	1.03×10^4 ^b	1.08	0.45	homogeneous
SI-10/6	1.51×10^4 ^a	1.52×10^4 ^b	1.09	0.65	homogeneous
SI-14/3	1.70×10^4 ^a	1.70×10^4 ^b	1.08	0.84	homogeneous
SI-5/6-5CN	3.15×10^4 ^e	3.15×10^4 ^e	1.04	0.14	spheres
SI-10/6-5CN	3.67×10^4 ^e	3.67×10^4 ^e	1.04	0.27	cylinders
SI-14/3-5CN	2.78×10^4 ^e	2.78×10^4 ^e	1.06	0.51	lamellae

^a Determined from vapor pressure osmometry. ^b Determined from membrane osmometry. ^c Determined from GPC. ^d Determined from ¹H NMR spectroscopy. ^e Calculated from stoichiometry.

accurate determination of the molecular weight of SI-5CN diblock copolymers via GPC was not possible unless information on the hydrodynamic volume of SI-5CN is available. In the absence of such information, in this study we have calculated the molecular weights of the three SI-5CN diblock copolymers synthesized using information on the degree of hydroxylation, and they are summarized in Table 1.

Sample Preparation. For transmission electron microscopy (TEM), specimens of the SI-5CN synthesized with a thickness of 1.0 nm were prepared by solvent casting from toluene in the presence of an antioxidant (Irganox 1010, Ciba-Geigy Group) and then slowly evaporating the majority of the solvent first at room temperature in a fume hood for 1 week and then at 10 °C above the glass transition temperature for 3 days in a vacuum oven to remove any residual solvent. For polarizing optical microscopy (POM), thin films of about 2–3 μ m in thickness were prepared by casting from a 1 wt % solution of toluene on a slide glass and then dried first in a fume hood and then in a vacuum oven.

Differential Scanning Calorimetry (DSC). Thermal transition temperatures of all specimens were determined by using a differential scanning calorimeter (Perkin-Elmer 7 Series), under a nitrogen atmosphere, at varying heating and/or cooling rates (1–20 °C/min).

Polarizing Optical Microscopy (POM). A hot-stage (TH-600 type, Linkham Scientific) microscope (Nikon, model Optiphot polXTP-11) with a camera, a programmable temperature controller, and photomicrographic grafting was used to take pictures, under cross-polarized light, of the film solvent cast on a slide glass.

Transmission Electron Microscopy (TEM). TEM images of specimens were taken at room temperature. The ultrathin sectioning (50–70 nm) was performed by cryoultramicrotomy at –80 °C, which is below the T_g of the PI block, for SI diblock copolymers and at room temperature for SI-5CN diblock copolymers. This was done using a Reichert Ultracut E low-temperature sectioning system. A transmission electron microscope (JEM1200EX 11, JEOL) operated at 120 kV was used to obtain images of the specimens stained with osmium tetroxide vapor for SI diblock copolymers or ruthenium tetroxide vapor for SI-5CN diblock copolymers.

Cloud Point Measurement. Cloud points of PS/(PI-5CN) mixtures were measured on a thin film, which was prepared by dissolving predetermined amounts of PS-4 and PI-4-5CN in toluene (ca. 10% solution). A few drops of this solution were placed on a slide glass and dried. The solvent was evaporated slowly at room temperature in a fume hood and then in a vacuum oven at an elevated temperature. The cloud point of a specimen was determined using laser light scattering. Specifically, a slide glass containing a sample was placed on the hot stage of the sample holder attached with a programmable temperature controller. A low-power He–Ne laser (wavelength of 635 nm) was used as the light source, and a photodiode was used as the detector. A sample was first heated to a temperature slightly (ca. 20 °C) above the cloud point (i.e., in the isotropic region), followed by slow cooling into the two-phase region where a change in light intensity was noticeable. The specimen was then heated again at a preset rate (0.5–5 °C/min), during which information on both temperature and the intensity of scattered light was recorded on a diskette. For each composition, cloud point measurements were repeated three to five times until data were reproducible, and a fresh sample was used for each experimental run. Seven to nine compositions from 10/90 to 90/10 blend ratios were used to measure cloud point.

Oscillatory Shear Rheometry. An Advanced Rheometric Expansion System (ARES) (Rheometric Scientific) was used in the oscillatory mode with parallel-plate fixtures (8 mm diameter). Dynamic frequency sweep experiments were conducted to measure the storage and loss moduli (G' and G'') as a function of angular frequency (ω) ranging from 0.03 to 100 rad/s at various temperatures. A fixed strain of 0.04 was used to ensure that measurements were taken well within the linear viscoelastic range of the materials investigated. The frequency sweep experiment at a preset temperature lasted for about 45 min, and the temperature control was accurate to within ± 1 °C. Dynamic temperature sweep experiments under isochronal conditions were also conducted at $\omega = 0.01$ rad/s during heating, for which temperature was increased 3 °C/min stepwise. All measurements were conducted under a nitrogen atmosphere in order to avoid oxidative degradation of the samples.

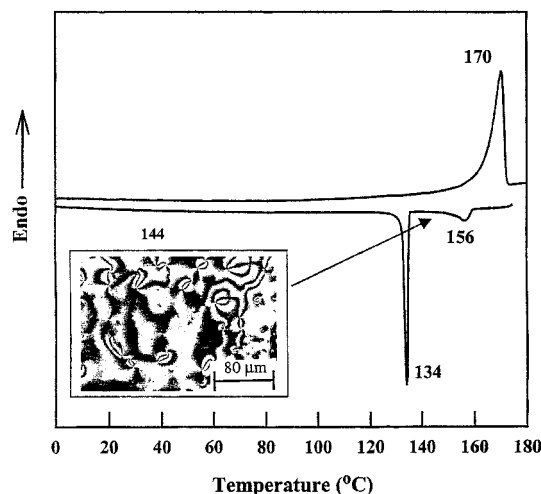


Figure 1. DSC traces of 5CN-COOH in the second heating and cooling cycles at a rate of 20 °C/min. The morphology of 5CN-COOH obtained from polarizing optical microscopy is also given in the inset.

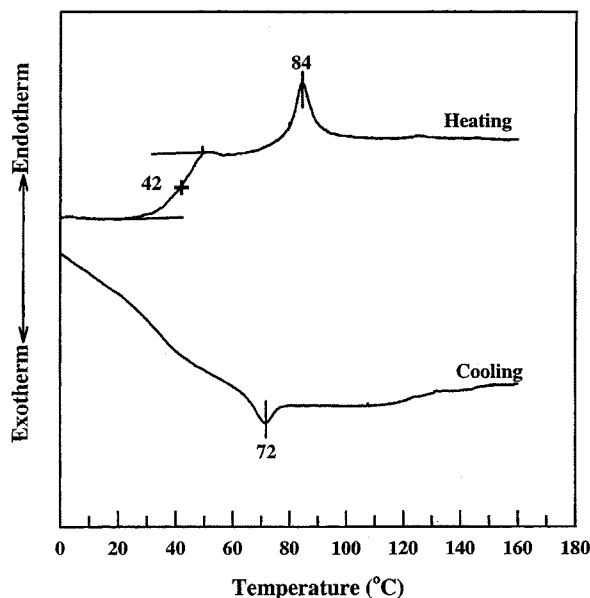


Figure 2. DSC traces of SI-5/6-5CN diblock copolymer in the second heating and cooling cycles at a rate of 20 °C/min.

Results and Discussion

Isotropization and LC Morphology of 5CN-COOH and SI-5CN. DSC traces for 5CN-COOH are given in Figure 1, showing that 5CN-COOH has the clearing temperature (T_{cl}) of 170 °C on heating and 156 °C on cooling. DSC traces for SI-5/6-5CN are given in Figure 2, showing that SI-5/6-5CN has the T_{cl} of 84 °C on heating and 72 °C on cooling. Comparison of Figure 1 with Figure 2 reveals that the T_{cl} of 5CN-COOH is decreased by about 90 °C, after being grafted onto the PI block of SI diblock copolymer SI-5/6. Similar observations, not presented here, were made for two other side-chain LC block copolymers, SI-10/6-5CN and SI-14/3-5CN. Later in this paper we will offer an explanation on the physical origin of the large difference in T_{cl} observed between the neat LC monomer 5CN-COOH and the side-chain LC block copolymer SI-5CN.

In the inset of Figure 1, a POM image of 5CN-COOH at 144 °C during the cooling cycle is given, showing two and four brushes which suggest the presence of nematic phase in the LC monomer 5CN-COOH. Figure 3 gives

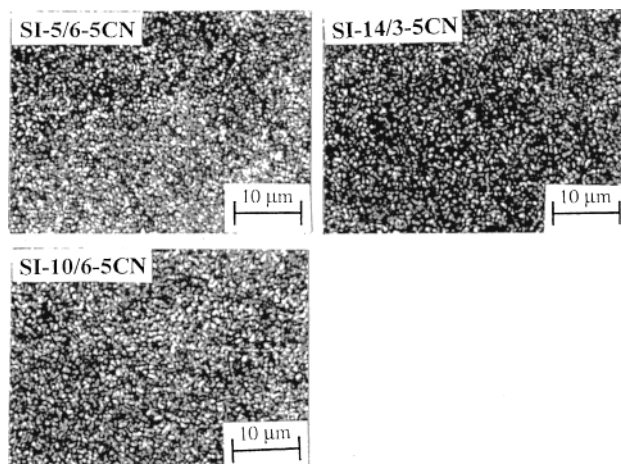


Figure 3. POM image, taken at room temperature, of SI-5/6-5CN, SI-14/3-5CN, and SI-10/6-5CN diblock copolymers.

POM images of the LC phase in SI-5/6-5CN, SI-10/6-5CN, and SI-14/3-5CN at room temperature. The POM images were taken using the specimens that were cast from toluene solution and dried at 65 °C for 3 days in a vacuum oven. In Figure 3 we observe that all three side-chain LC diblock copolymers have a nematic mesophase, which looks very similar to that observed in a segmented main-chain LC homopolymer.²⁸ It is interesting to note that the sizes of nematic phase in the side-chain LC diblock copolymers (Figure 3) are very small compared to those in the neat LC monomer 5CN-COOH (Figure 1).

Microdomain Structure and Microphase Separation Transition (MST) in SI-5CN. In a previous paper,²⁷ we reported that the three SI diblock copolymers (SI-5/6, SI-10/6, and SI-14/3) are homogeneous over the entire range of temperatures tested. In view of the fact that MST may be induced by increasing the molecular weight of a homogeneous block copolymer, in the present study we investigated whether MST was induced after an LC monomer 5CN-COOH was grafted onto the PI block of the SI diblock copolymer. For this, we used both oscillatory shear rheometry and TEM.

Figure 4 gives $\log G'$ vs $\log G''$ plots, which Neumann et al.²⁹ referred to as Han plots, for SI-14/3-5CN at various temperatures. It is seen from the inset of Figure 4 that SI-14/3-5CN forms lamellar microdomains at room temperature, indicating that microphase separation was induced by the grafting of 5CN-COOH onto the polyisoprene (PI) block of a homogeneous block copolymer SI-14/3, and the slope of the $\log G'$ vs $\log G''$ plot in the terminal region is less than 2 over the entire range of temperatures tested. Han and co-workers³⁰ advocate that the T_{ODT} of a block copolymer can be determined by the *threshold* temperature at which the $\log G'$ vs $\log G''$ plot, having a slope of 2 in the terminal region, begins to show temperature independence. According to such a rheological criterion, we conclude from Figure 4 that SI-14/3-5CN has T_{ODT} higher than 240 °C, the highest experimental temperature employed. Also given in the inset of Figure 4 are the results of the isochronal dynamic temperature sweep experiments at $\omega = 0.01$ rad/s. It is seen that values of G' remain very large over the entire range of temperatures tested. According to the literature,³¹ the T_{ODT} of a block copolymer can be determined by identifying a temperature at which G' begins to drop precipitously in isochronal dynamic temperature sweep experiment. We

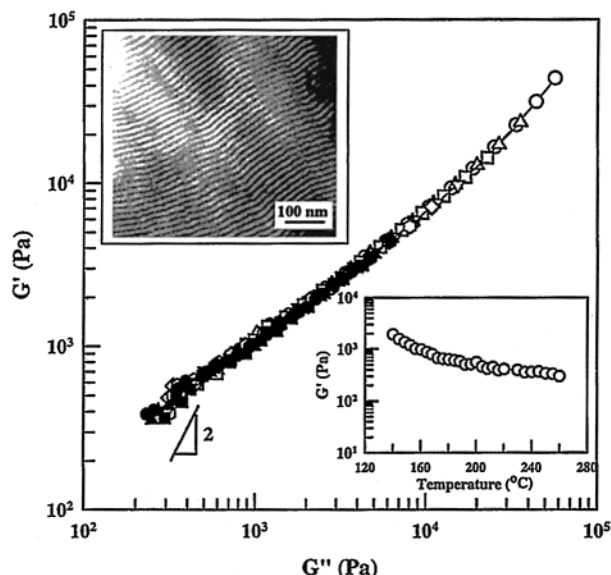


Figure 4. Log G' vs log G'' plots for SI-14/3-5CN diblock copolymer at various temperatures: (○) 160, (△) 170, (□) 180, (▽) 190, (◇) 200, (○) 210, (●) 220, (▲) 230, and (■) 240 °C. The inset at the lower right-hand side describes variations of G' with temperature during isochronal dynamic temperature sweep experiments of SI-14/3-5CN diblock copolymer at $\omega = 0.01$ rad/s. The inset at the upper left-hand side gives a TEM image, taken at room temperature, of SI-14/3-5CN.

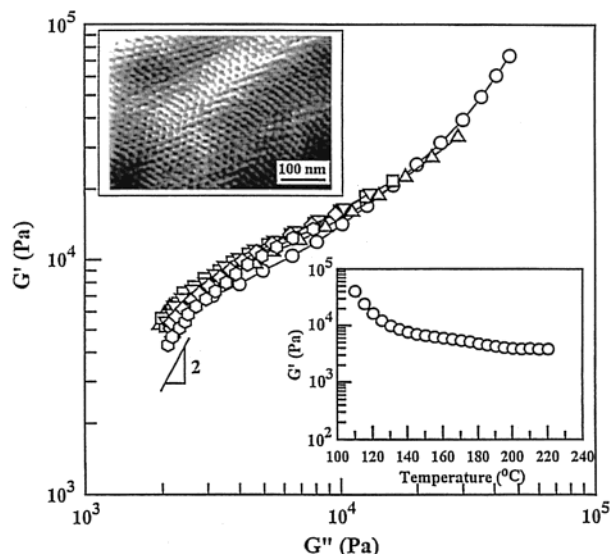


Figure 5. Log G' vs log G'' plots for SI-10/6-5CN diblock copolymer at various temperatures: (○) 130, (△) 150, (□) 170, (▽) 180, (◇) 200, and (○) 220 °C. The inset at the lower right-hand side describes variations of G' with temperature during isochronal dynamic temperature sweep experiments of SI-10/6-5CN diblock copolymer at $\omega = 0.01$ rad/s. The inset at the upper left-hand side gives a TEM image, taken at room temperature, of SI-10/6-5CN.

thus conclude from Figure 4 that the T_{ODT} of SI-14/3-5CN is higher than 260 °C. This conclusion is consistent with that drawn from the log G' vs log G'' plot.

Figure 5 gives log G' vs log G'' plots for SI-10/6-5CN at various temperatures. It is seen from the inset of Figure 5 that SI-10/6-5CN forms hexagonally packed cylindrical microdomains at room temperature, indicating that microphase separation was induced by the grafting of 5CN-COOH onto the polyisoprene (PI) block of a homogeneous block copolymer SI-10/6. Notice in Figure 5 that the slope of the log G' vs log G'' plot

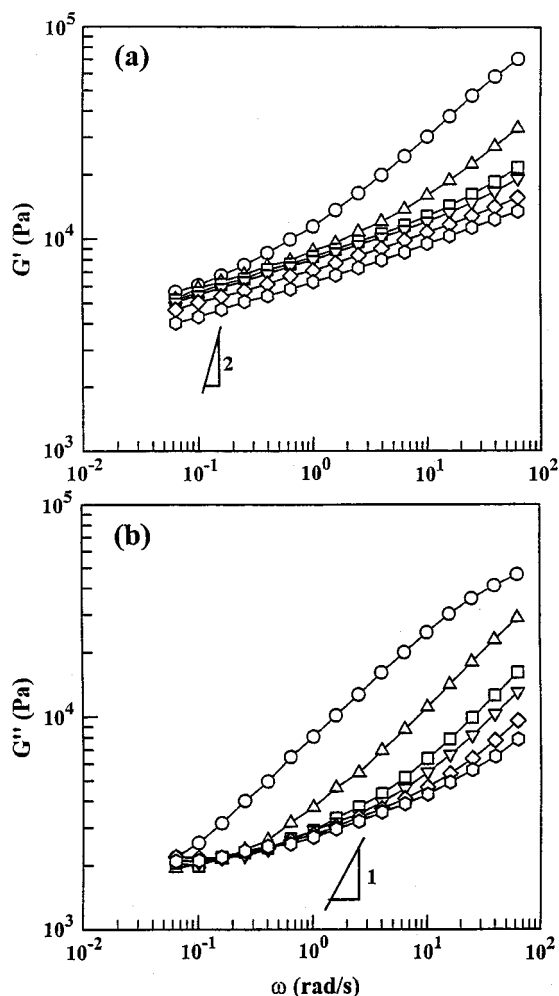


Figure 6. (a) Plots of log G' vs log ω and (b) plots of log G'' vs log ω for SI-10/6-5CN diblock copolymer at various temperatures: (○) 130, (△) 150, (□) 170, (▽) 180, (◇) 200, and (○) 220 °C.

appears to be close to 2 at or near the lowest value of G' experimentally measured, while there exists *no* threshold temperature at which the log G' vs log G'' plot begins to show temperature independence; i.e., the log G' vs log G'' plot varies with temperature up to the highest experimental temperature employed (220 °C). Figure 6 gives plots of log G' vs log ω and log G'' vs log ω for SI-10/6-5CN at various temperatures, showing that SI-10/6-5CN exhibits solidlike rheological responses even at the highest experimental temperature employed, 220 °C. Also given in the inset of Figure 5 are the results of the isochronal dynamic temperature sweep experiments at $\omega = 0.01$ rad/s, showing that values of G' remain constant and there exists no critical temperature at which G' begins to drop precipitously. This observation leads us to conclude that the T_{ODT} of SI-10/6-5CN is much higher than 220 °C, which is in agreement with the conclusion drawn from the log G' vs log G'' plot.

Figure 7 gives log G' vs log G'' plots for SI-5/6-5CN at various temperatures. It is seen from the inset of Figure 7 that SI-5/6-5CN forms spherical microdomains, indicating that microphase separation was induced by the grafting of 5CN-COOH onto the polyisoprene (PI) block of a homogeneous block copolymer SI-5/6. It is of interest to observe in Figure 7 that the log G' vs log G'' plot in the terminal region begins to have a slope of 2

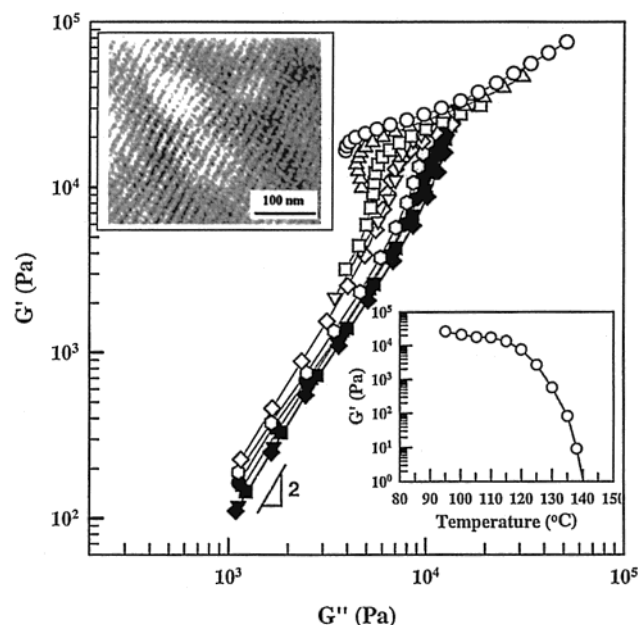


Figure 7. Log G' vs log G'' plots for SI-5/6-5CN diblock copolymer at various temperatures: (○) 110, (△) 120, (□) 130, (▽) 137, (◇) 140, (○) 143, (●) 149, (▲) 152, (■) 155, (▼) 160, and (◆) 165 °C. The inset describes variations of G' with temperature during isochronal dynamic temperature sweep experiments of SI-5/6-5CN diblock copolymer at $\omega = 0.01$ rad/s. The inset at the upper left-hand side gives a TEM image, taken at room temperature, of SI-5/6-5CN.

at 140 °C, makes a parallel shift downward until reaching 155 °C, and then becomes virtually independent of temperature at 155 °C and higher. It should be mentioned that the SI-5/6-5CN diblock copolymer specimens employed for the rheological measurements, the results of which are summarized in Figure 7, were annealed at 90 °C for 1 week. Han and co-workers³² have shown that during heating a sphere-forming block copolymer first undergoes lattice disordering transition forming “disordered micelles” and then a demicellization transition transforming into the micelle-free homogeneous phase. However, during cooling it first undergoes a micellization transition forming “disordered micelles” from the micelle-free homogeneous phase and then a lattice ordering transition forming the body-centered-cubic (bcc) phase with long-range order. They have taken the position that “disordered micelles” are stable, and the lattice disordering/ordering transition (LDOT) and demicellization/micellization transition (DMT) are thermodynamically reversible. According to such a criterion, from Figure 7 we conclude that SI-5/6-5CN has the LDOT temperature (T_{LDOT}) at 140 °C and the DMT temperature (T_{DMT}) at 155 °C. Also given in Figure 7 are the results of isochronal dynamic temperature sweep experiments for SI-5/6-5CN, showing that G' begins to drop rapidly at ca. 120 °C and has a very low value at ca. 140 °C, which corresponds to T_{LDOT} in the log G' vs log G'' plot.

Very recently, Dormidontova and Lodge³³ extended Semenov's strong-segregation theory^{34,35} for asymmetric block copolymers. Interestingly, they were able to confirm the experimental results³² of the existence of disordered micelles in sphere-forming diblock copolymers at elevated temperatures, while previous mean-field calculations could not.^{36–39} Dormidontova and Lodge concluded that disordered micelles are part of the disordered phase, which is at variance with experimen-

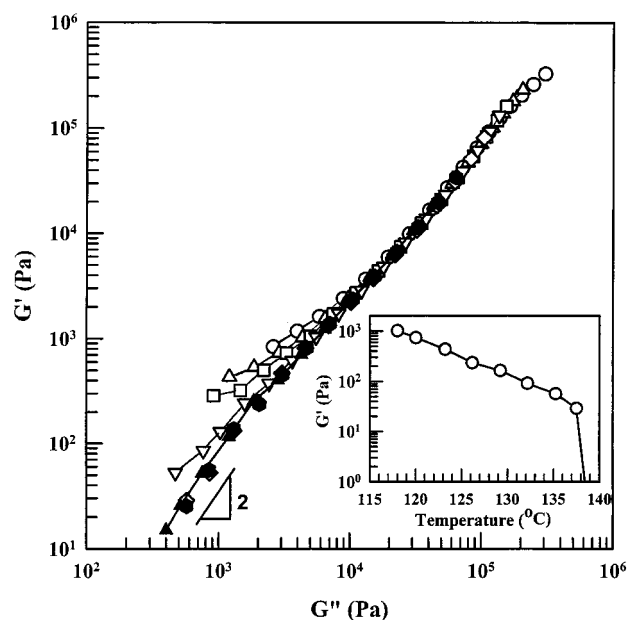


Figure 8. Log G' vs log G'' plots for SI-14/3-5CN-30 diblock copolymer at various temperatures: (○) 120, (△) 125, (□) 130, (▽) 135, (◇) 138, (○) 140, (●) 145, and (▲) 150 °C. The inset describes variations of G' with temperature during isochronal dynamic temperature sweep experiments of SI-14/3-5CN-30 diblock copolymer at $\omega = 0.01$ rad/s.

tal observations.³² The discrepancy between theory and experiment needs to be resolved in the future. While the mean-field approach employed by Dormidontova and Lodge, which is based on many assumptions made for simplicity, has been successful in explaining certain physical phenomena occurring in block copolymers, we are of the opinion that it cannot be expected to explain every conceivable physical phenomena occurring in block copolymers. Thus, it is worth looking into other theoretical approaches to predict DMT in sphere-forming block copolymers.

Grafting of 5CN-COOH onto the PI block of an SI diblock copolymer not only increases the molecular weight of the resulting block copolymer SI-5CN substantially but also changes block composition. For instance, SI-14/3 has $M_n = 1.7 \times 10^4$ g/mol and a PS weight fraction (w_{PS}) of 0.83, while SI-14/3-5CN has $M_n = 2.78 \times 10^4$ g/mol and $w_{PS} = 0.51$ when all 1,2- and 3,4-addition of PI blocks of SI-14/3 were grafted with 5CN-COOH (see Table 1). It should be mentioned that grafting of 5CN-COOH onto the PI block of SI-14/3 also changed segmental interactions between the constituent blocks; i.e., the interaction parameter χ between PS and PI blocks in SI-14/3 would be different from that between PS and PI-5CN blocks in SI-14/3-5CN.

Figure 8 gives log G' vs log G'' plots for SI-14/3-5CN-30 with 30% of 1,2- and 3,4-addition of the PI block of SI-14/3 being grafted with 5CN-COOH, and Figure 9 gives log G' vs log G'' plots for SI-14/3-5CN-70 with 70% of 1,2- and 3,4-addition of the PI blocks of SI-14/3 being grafted with 5CN-COOH. The partially grafted SI-14/3-5CN-30 and SI-14/3-5CN-70 were prepared by first controlling the degree of hydroxylation when an SI-14/3 was hydroborated followed by oxidation; i.e., during the hydroxylation, 30% of 1,2- and 3,4-addition of the PI block of SI-14/3 was hydroxylated yielding SI-14/3-OH-30 and 70% of 1,2- and 3,4-addition of the PI block of SI-14/3 was hydroxylated yielding SI-14/3-OH-70. Then, LC monomer, 5CN-COOH, was grafted on all of the

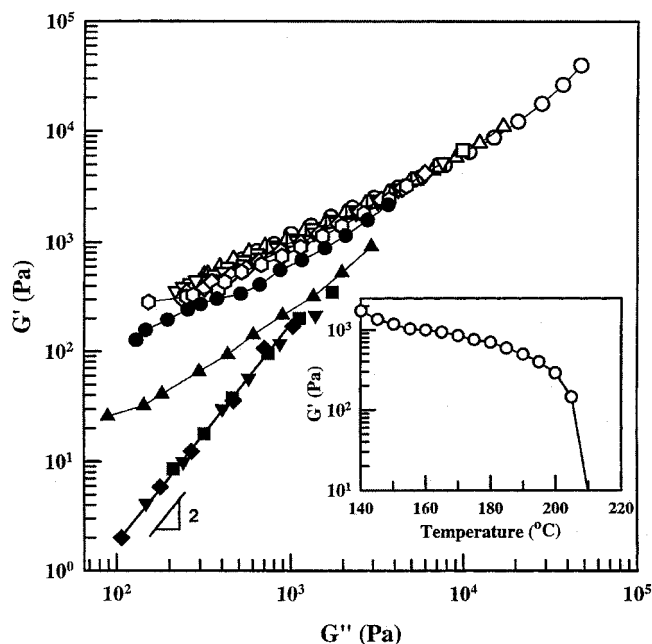


Figure 9. Log G' vs log G'' plots for SI-14/3-5CN-70 diblock copolymer at various temperatures: (○) 150, (△) 170, (□) 180, (▽) 185, (◇) 190, (○) 195, (●) 200, (▲) 205, (■) 210, (▼) 215, and (◆) 220 °C. The inset describes variations of G' with temperature during isochronal dynamic temperature sweep experiments of SI-14/3-5CN-70 diblock copolymer at $\omega = 0.01$ rad/s.

hydroxyl groups in the respective diblock copolymers, SI-14/3-OH-30 and SI-14/3-OH-70. The readers are reminded that the reaction scheme for the graft reactions and the experimental procedures employed are presented in the Experimental Section. Note that SI-14/3-5CN-30 has $w_{PS} = 0.69$ (thus, it is expected to have hexagonally packed cylindrical microdomains) and SI-14/3-5CN-70 has $w_{PS} = 0.56$ (thus, it is expected to have lamellar microdomains). Notice in Figure 8 the temperature dependence of the log G' vs log G'' plot for SI-14/3-5CN-30 and in Figure 9 the temperature dependence of the log G' vs log G'' plot for SI-14/3-5CN-70 in that the log G' vs log G'' plots in both figures do not exhibit a parallel shift, quite different from the log G' vs log G'' plot for SI-5/6-5CN given in Figure 7. This is because both SI-14/3-5CN-30 ($w_{PS} = 0.69$) and SI-14/3-5CN-70 ($w_{PS} = 0.56$) are expected to undergo ODT, while SI-5/6-5CN ($w_{PS} = 0.14$) is expected to undergo LDOT followed by DMT. It should be mentioned that the PI-5CN-30 block in SI-14/3-5CN and the PI-5CN-70 block in SI-14/3-5CN are random copolymers consisting of PI-5CN and unreacted PI. The log G' vs log G'' plots given in Figures 8 and 9 indicate that SI-14/3-5CN-30 has the T_{ODT} of 138 °C and SI-14/3-5CN-70 has the T_{ODT} of 210 °C, which are in good agreement with the values of T_{ODT} that can be determined from the isochronal dynamic temperature sweep experiments (see the insets of Figures 8 and 9). In other words, the T_{ODT} of SI-14/3-5CN is increased as the amount of 5CN-COOH grafted onto the PI block is increased.

Complex Viscosity of SI-5CN. Figure 10 gives logarithmic plots of complex viscosity $|\eta^*|$ vs ω for SI-14/3-5CN at temperatures ranging from 160 to 240 °C. Note that values of $|\eta^*|$ were calculated using the relationship $|\eta^*| = [(G'/\omega)^2 + (G''/\omega)^2]^{1/2}$. In Figure 10 we observe that $|\eta^*|$ exhibits a strong frequency dependence over the entire range of temperatures investi-

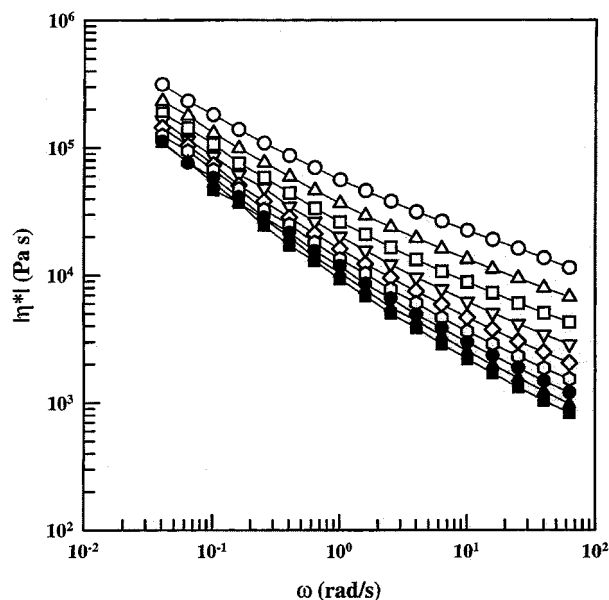


Figure 10. Plots of log $|\eta^*|$ vs log ω for SI-14/3-5CN at various temperatures: (○) 160, (△) 170, (□) 180, (▽) 190, (◇) 200, (○) 210, (●) 220, (▲) 230, and (■) 240 °C.

gated, behavior often observed in highly filled polymer systems⁴⁰ and also microphase-separated block copolymers.⁴¹ The above observation reinforces the conclusion drawn from the log G' vs log G'' plots given in Figure 4 that SI-14/3-5CN has microdomains over the entire range of temperatures tested from 160 to 240 °C. Similar results, not presented here, were obtained for SI-10/6-5CN at temperatures ranging from 110 to 220 °C. For SI-14/3-5CN-70, in which only 70% of 1,2- and 3,4-addition of the PI block in SI-14/3 are grafted with LC monomer 5CN-COOH, we observed that a strong frequency dependence of $|\eta^*|$, not presented here, became weaker at 205 °C and then exhibited Newtonian behavior at 215 and 220 °C, behavior usually observed for low-molecular-weight homopolymers. The above observation suggests that all microdomains in SI-14/3-5CN-70 melt away at 215 °C and SI-14/3-5CN-70 becomes a homogeneous random copolymer at 215 °C and higher temperatures. This observation is consistent with the conclusion drawn from Figure 9 that SI-14/3-5CN-70 undergoes ODT at 210 °C.

Figure 11 gives log $|\eta^*|$ vs log ω plots for SI-5/6-5CN at temperatures ranging from 110 to 165 °C. Note that the temperature dependence of $|\eta^*|$ for SI-5/6-5CN given in Figure 11 is quite different from that for SI-14/3-5CN given in Figure 10. The following observations are worth noting in Figure 11. We observe a strong frequency dependence of $|\eta^*|$ at 110–130 °C, a manifestation that SI-5/6-5CN is microphase-separated. We observe Newtonian behavior at low values of ω when the temperature is increased to 146 °C and higher, suggesting that SI-5/6-5CN has lost long-range order. However, from Figure 11 we cannot determine the T_{LDOT} and T_{DMT} of SI-5/6-5CN. It should be pointed out that the frequency dependence of $|\eta^*|$ for SI-5/6-5CN at $T > T_{DMT}$ (155 °C in accordance with Figure 7) originates from chain entanglement. Note that the molecular weight ($M_n = 3.15 \times 10^4$ g/mol) of SI-5/6-5CN is greater than the entanglement molecular weight (ca. 1.8×10^4 g/mol) of PS. Although the molecular weight of PS block in SI-5/6-5CN is certainly lower than the entanglement

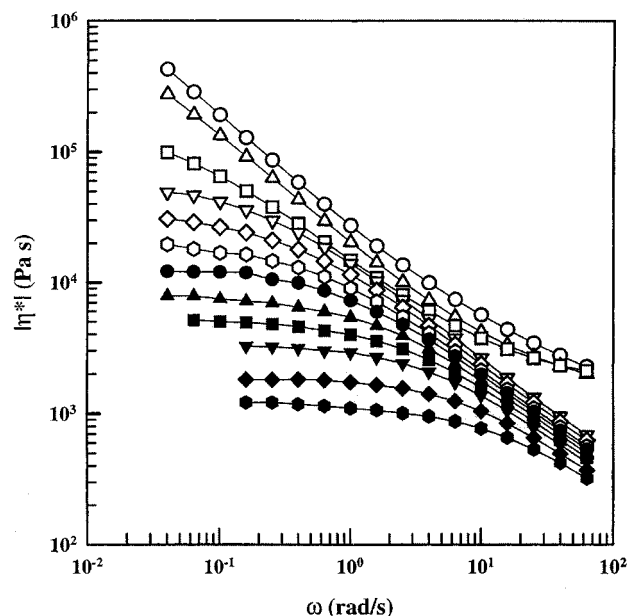


Figure 11. Plots of $\log |\eta^*|$ vs $\log \omega$ for SI-5/6-5CN at various temperatures: (○) 110, (△) 120, (□) 130, (▽) 137, (◇) 140, (○) 143, (●) 146, (▲) 149, (■) 152, (▼) 155, (◆) 160, and (●) 165 °C.

Table 2. Molecular Characteristics of Three PI and Three PI-5CN Synthesized in This Study

sample code	M_n (g/mol)	M_w/M_n^c	deg of LC grafting (%) ^d
PI-4	3 600 ^a	1.09	0
PI-13	14 300 ^b	1.05	0
PI-100	91 000 ^b	1.05	0
PI-4-5CN	18 000 ^e	1.08	100
PI-13-5CN	71 900 ^e	1.08	100
PI-100-5CN	470 000 ^e	1.09	100

^a Determined from vapor pressure osmometry. ^b Determined from membrane osmometry. ^c Determined from GPC. ^d Determined from ¹H NMR and FTIR spectroscopies. ^e Calculated from stoichiometry.

molecular weight of PS, the molecular weight of PI-5CN block is believed to be greater than the entanglement molecular weight of PI. We wish to add that SI-5/6-5CN in the homogeneous state (i.e., at $T > T_{DMT}$) has a comblike molecular architecture in that the PI block has pendant groups of large 5CN-COOH molecules as side chains. At present, it is very difficult to speculate how such large pendant groups grafted onto the PI block of an SI diblock copolymer might affect the rheological behavior of SI-5/6-5CN in the homogeneous state (i.e., at $T > T_{DMT}$).

Hydrogen-Bonding Effect on the Clearing Temperature of 5CN-COOH. In Figures 1 and 2 we have shown that the T_{cl} of the LC phase in SI-5/6-5CN is only 84 °C while the T_{cl} of LC monomer 5CN-COOH is 170 °C. To investigate whether the length of the PI block in SI-5/6-5CN might affect the T_{cl} of its LC phase, we synthesized homopolymer PIs having three different molecular weights (M_n): 3600, 14 300, and 91 000 g/mol (see Table 2). LC monomer 5CN-COOH was grafted onto each of the PIs, using the procedures described in the Experimental Section, yielding PI-4-5CN, PI-13-5CN, and PI-100-5CN. The DSC traces for the three PI-5CNs and also for the neat homopolymer PI, PI-4, are given in Figure 12. It should be mentioned that the glass transition temperature ($T_g = -25$ °C) of the PI, which was synthesized in THF yielding 34% 1,2-addition, 59%

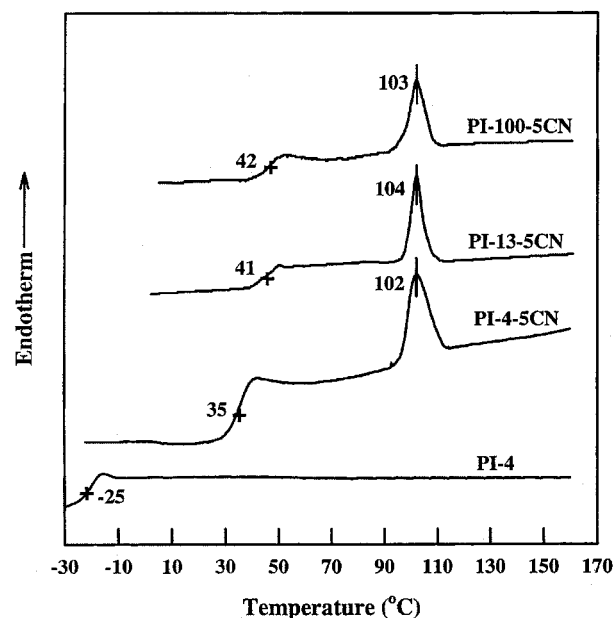
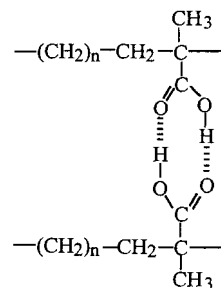


Figure 12. DSC traces for PI-4, PI-4-5CN, PI-13-5CN, and PI-100-5CN in the second heating at a rate of 20 °C/min, in which PI-4 has $M_n = 3600$ g/mol, PI-13 has $M_n = 14\,300$ g/mol, and PI-100 has $M_n = 91\,000$ g/mol.

3,4-addition, and 7% 1,4-addition, is much higher than that ($T_g = -60$ °C) of the PI that was synthesized in cyclohexane, yielding 94% 1,4-addition and 6% 3,4-addition. It is seen in Figure 12 that all three PI-5CNs have virtually an identical clearing temperature, $T_{cl} \approx 103$ °C, leading us to conclude that the length of the PI chain has no effect on the T_{cl} of PI-5CN. It should be remembered that 5CN-COOH has the T_{cl} of 170 °C (see Figure 1). Therefore, we must look into other factor(s) that might explain the reason that the T_{cl} of the LC phase in SI-5/6-5CN is 84 °C (see Figure 2), while the T_{cl} of LC monomer 5CN-COOH is 170 °C (see Figure 1).

In view of the fact that ethylene-*co*-methacrylic acid, for instance, forms hydrogen bonding,



it seemed reasonable to speculate on the possibility that the carboxyl end groups in 5CN-COOH might form hydrogen bonding. To confirm such a possibility, we conducted FTIR measurements for PI-5CN and 5CN-COOH specimens, and the FTIR spectra are given in Figure 13. It is seen that the IR spectrum of LC monomer 5CN-COOH exhibits an absorption peak at 1700 cm^{-1} representing the *hydrogen-bonded* carbonyl group and the IR spectrum of PI-5CN exhibits an absorption peak at 1730 cm^{-1} representing the *free* carbonyl group.⁴² That is, after the coupling reaction between the hydroxyl groups in PI-OH and the carboxyl groups in 5CN-COOH, the resulting PI-5CN no longer has hydrogen bonding, while the LC monomer 5CN-

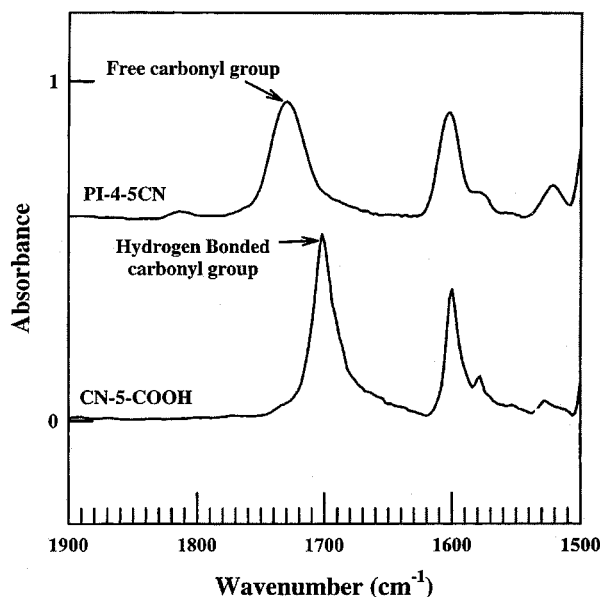


Figure 13. IR spectra for 5CN-COOH showing hydrogen-bonded carbonyl group and for PI-4-5CN showing only free carbonyl group; i.e., the hydrogen bonding present in the neat LC monomer 5CN-COOH is disrupted after the grafting to the polyisoprene PI-4.

COOH has hydrogen bonding. Thus, we conclude the high T_{cl} (ca. 170 °C) of 5CN-COOH (see Figure 1) compared to the T_{cl} (ca. 86 °C) of SI-5CN (see Figure 2) originates from the presence of hydrogen bonding in 5CN-COOH.

There still may be another reason why SI-5CN has a lower T_{cl} compared to that of 5CN-COOH. Namely, the PI backbone of SI-5CN might hinder the ordering of the LC monomer 5CN-COOH that is pendent, as side chain, to the PI block. Since the main chain, consisting of PS and PI blocks, of SI-5CN is amorphous, it may still want to remain as a coiled chain even after the grafting of LC monomer 5CN-COOH onto the PI block.

Segmental Interactions between PS and PI-5CN.

In Figures 4, 5, and 7 we have shown that lamellar, hexagonally packed cylindrical, or spherical microdomains are introduced, depending upon block composition, into the side-chain LC diblock copolymer, SI-5CN, after LC monomer 5CN-COOH was grafted onto the PI block of a *homogeneous* SI diblock copolymer. The chemical modification of SI diblock copolymer has brought about three changes: an increase in molecular weight, block composition f , and segmental interaction parameter χ . In this study, we investigated segmental interactions between PS and PI-5CN using cloud point measurements. For this, we synthesized a homopolymer PI having $M_n = 3500$ g/mol (PI-4) and then prepared a series of PI-4-5CNs having varying amounts of LC monomer. Also, we synthesized a homopolymer PS having $M_n = 4100$ g/mol (PS-4). The molecular characteristics of PS-4, PI-4, and the four PI-4-5CNs synthesized are summarized in Table 3, in which the numbers 5, 50, 80, and 100 after 5CN refer to the percent of LC content in each PI-4-5CN.

Figure 14 gives DSC traces for PI-4 and the four PI-4-5CNs, showing glass transition temperature (T_g) and endothermic peak representing clearing temperature (T_{cl}). It is seen that PI-4-5CN-5 (5% LC content) remains a glassy polymer, indicating that the amount of LC monomer grafted is not sufficient to give rise to liquid crystallinity. To facilitate our discussion below, the

Table 3. Molecular Characteristics of the PI-5CNs Synthesized for Cloud Point Measurement

sample code	M_n (g/mol)	M_w/M_n^a	deg of LC grafting (%) ^b
PS-4	4 100 ^a	1.05	0
PI-4	3 600 ^c	1.09	0
PI-4-5CN-5	4 500 ^d	1.09	5
PI-4-5CN-50	11 600 ^d	1.09	50
PI-4-5CN-80	16 200 ^d	1.07	80
PI-4-5CN-100	18 000 ^d	1.08	100

^a Determined from GPC. ^b Determined from ¹H NMR and FTIR spectroscopies. ^c Determined from vapor pressure osmometry. ^d Calculated from stoichiometry.

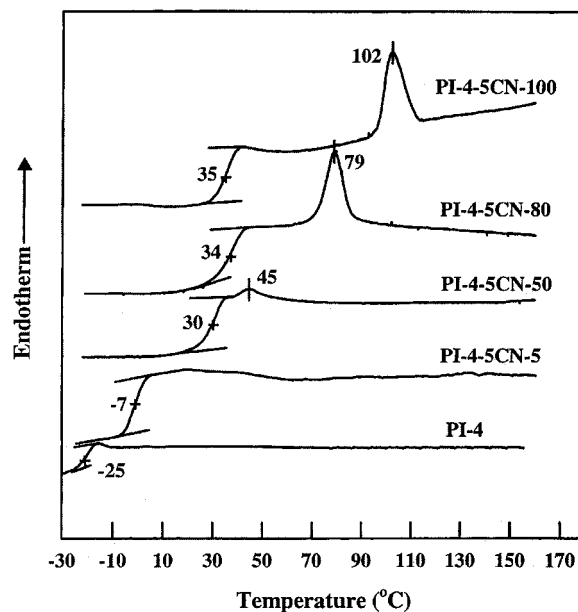


Figure 14. DSC traces for PI-4, PI-4-5CN-5, PI-4-5CN-50, PI-4-5CN-80, and PI-4-5CN-100 in the second heating at a rate 20 °C/min, in which PI-4 refers to the molecular weight ($M_n = 3600$ g/mol) of polyisoprene, and the numbers 5, 50, 80, and 100 next to 5CN refer to the percent of LC monomer grafted onto PI-4 with $M_n = 3600$ g/mol.

dependence of T_g and T_{cl} of PI-5CN on the amount of LC grafted is summarized in Figure 15. It is seen that T_g first increases with increasing amount of the LC monomer grafted and then levels off at about 50% of the LC monomer grafted, while T_{cl} increases linearly with the amount of the LC monomer grafted.

Using the homopolymers PS-4, PI-4, and PI-4-5CNs summarized in Table 3, we prepared, via solution casting from toluene, binary blends—(PS-4)/(PI-4), (PS-4)/(PI-4-5CN-5), (PS-4)/(PI-4-5CN-50), (PS-4)/(PI-4-5CN-80), and (PS-4)/(PI-4-5CN-100)—with varying compositions and measured cloud point of each blend using light scattering. The Experimental Section describes the procedures used to measure cloud point. Figure 16 gives binodal curves determined from the cloud point measurements for (PS-4)/(PI-4), (PS-4)/(PI-4-5CN-5), (PS-4)/(PI-4-5CN-50), (PS-4)/(PI-4-5CN-80), and (PS-4)/(PI-4-5CN-100) blends. The following observations are worth noting in Figure 16. (i) All binary blends show upper critical solution temperature (UCST). (ii) The critical composition, which is about 0.5 for (PS-4)/(PI-4) blends, is shifted toward the right-hand side as the amount of the LC monomer grafted is increased as expected, because the molecular weight of PI-4-5CN block is increased with increasing amount of LC monomer grafted. (iii) The critical temperature is increased

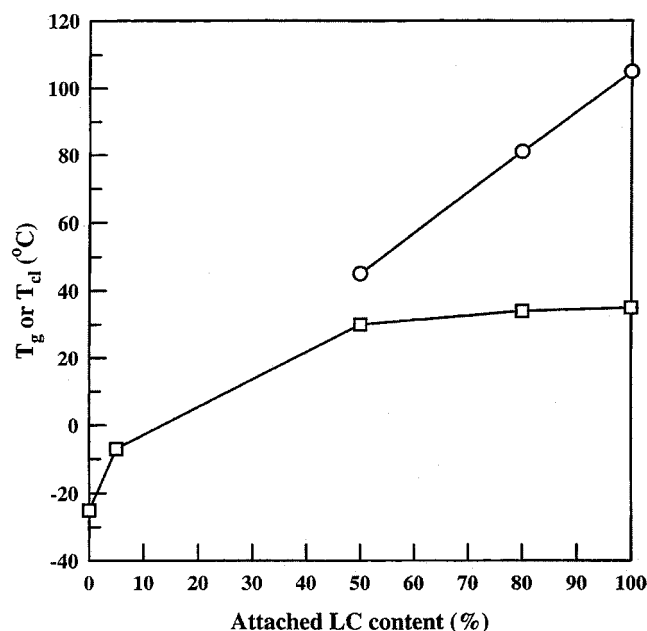


Figure 15. Plots of T_g (\square) and T_d (\circ) of PI-5CN vs the amount of LC monomer grafted onto PI, showing that T_g levels off beyond ca. 50% LC grafting, while T_d increases linearly with the amount of LC monomer grafted.

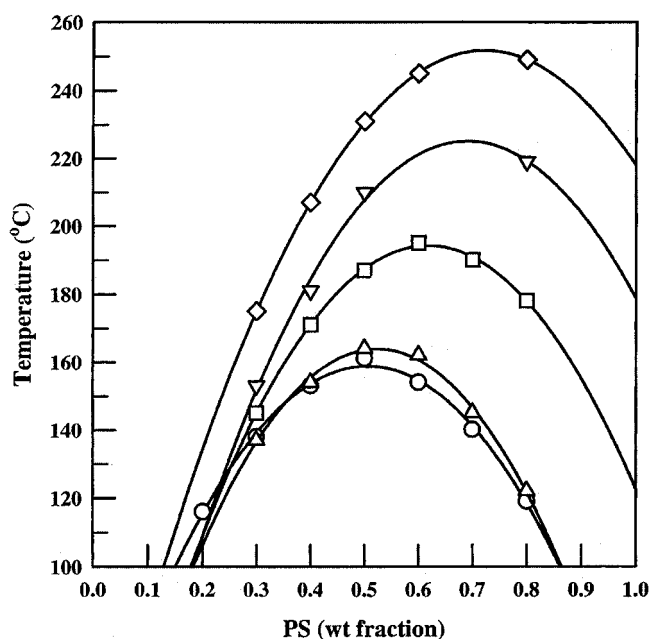


Figure 16. Binodal curves constructed from cloud point measurements for (\circ) (PS-4)/(PI-4) binary mixtures, (Δ) (PS-4)/(PI-4-5CN-5) binary mixtures, (\square) (PS-4)/(PI-4-5CN-50) binary mixtures, (∇) (PS-4)/(PI-4-5CN-80) binary mixtures, (\diamond) (PS-4)/(PI-4-5CN-100) binary mixtures, in which the numbers 5, 50, 80, and 100 next to 5CN refer to the percent of LC monomer grafted onto PI-4 with $M_n = 3600$ g/mol.

with increasing amount of LC monomer grafted, indicating that repulsive segmental interactions between PS-4 and PI-4-5CN increase with increasing amount of LC monomer grafted. As mentioned above, two other factors, an increase in molecular weight M_n (from 2.08×10^4 g/mol for 30% LC monomer content to 2.57×10^4 g/mol for 70% LC monomer content and to 2.78×10^4 g/mol for 100% LC monomer content) and a change in block composition (i.e., a decrease in the weight fraction w_{PS} of PS from 0.69 for 30% LC monomer content to 0.56 for 70% LC monomer content and to 0.51 for 100%

LC monomer content) also must have played an important role in the increase of T_{ODT} of SI-14/3-5CN, experimentally observed, as the amount of LC monomer grafted is increased.

We can calculate the segmental interaction parameter for each (PS-4)/(PI-4-5CN) pair using the binodal curves given in Figure 16 if the Flory-Huggins theory is assumed to be applicable to the (PS-4)/(PI-4-5CN) pair at temperatures above the T_{cl} of PI-4-5CN. For this, we need the temperature dependence of specific volume for PI-4-5CN-5, PI-4-5CN-50, PI-4-5CN-80, and PI-4-5CN-100. In this study we have determined, via PVT measurement, the specific volume of PI-4-5CN-100 to be⁴³

$$V_{PI-4-5CN-100} = 1.2805 + 3.68 \times 10^{-4}(T - 273) \text{ (cm}^3\text{/g)} \quad (1)$$

at temperatures above the T_{cl} of PI-4-5CN-100. Using the specific volume of PS given by⁴⁴

$$V_{PS} = 0.9217 + 5.412 \times 10^{-4}(T - 273) + 1.687 \times 10^{-7}(T - 273)^2 \text{ (cm}^3\text{/g)} \quad (2)$$

together with eq 1, we have obtained the following expression for the segmental interaction parameter

$$\alpha_{PS/(PI-4-5CN-100)} = -0.3052 \times 10^{-3} + 0.2744/T \quad (3)$$

for the (PS-4)/(PI-4-5CN-100) pair, where α is related to the Flory-Huggins interaction parameter χ by $\chi = V_{ref}\alpha$ with V_{ref} being the reference volume. Since there are different ways of defining V_{ref} , one may obtain different expressions for $\chi(T)$ depending upon the choice of V_{ref} . For instance, one can define V_{ref} by the molar volume of one of the constituent components or by the geometric average of the molar volumes of the constituent components.^{30b} When choosing the molar volume of one of the constituent components to be V_{ref} , it is suggested that V_{ref} be chosen to be the molar volume of the component having the highest molecular weight of the constituent components. For comparison, let us choose the molar volume of PI-4-5CN as V_{ref} , $V_{ref} = 484$ cm³/mol. We then have

$$\chi_{PS/(PI-5CN)} = -0.1471 + 132.8/T \quad (4)$$

On the other hand, using the binodal curve for (PS-4)/(PI-4) pair given in Figure 16, we obtain

$$\alpha_{PS/PI} = -0.2939 + 0.3174/T \quad (5)$$

which becomes

$$\chi_{PS/PI} = -0.0335 + 36.24/T \quad (6)$$

in which the molar volume of styrene was chosen to be V_{ref} , $V_{ref} = 114.15$ cm³/mol. Comparison of eq 4 with eq 6 indicates that the temperature coefficient of $\chi_{PS/(PI-5CN)}$ is much greater than that of $\chi_{PS/PI}$, suggesting that the temperature dependence of repulsive segmental interactions between PS and PI-5CN is much greater than that between PS and PI. Note that at 200 °C, for instance, $\chi_{PS/(PI-5CN)} = 0.1337$ from eq 4 and $\chi_{PS/PI} = 0.0431$ from

eq 6, indicating that the PS/(PI-5CN) pair is highly segregated compared to the PS/PI pair.

Concluding Remarks

In this study, we have succeeded in inducing a microdomain structure from a *homogeneous* SI block copolymer by attaching an LC monomer 5CN-COOH, yielding a side-chain LC block copolymer SI-5CN. By judiciously controlling the block length ratio of SI diblock copolymer, we were able to observe lamellar microdomains, hexagonally packed cylindrical microdomains, or spherical microdomains in a body-centered-cubic lattice. Because in general the molecular weight of an LC monomer is rather high (e.g., 5CN-COOH has $M_w = 309$ g/mol), it is not easy to observe MST in a side-chain LC block copolymer, before thermal degradation may occur, after an LC monomer is grafted onto a block copolymer *unless* the molecular weight of a block copolymer is carefully controlled. In our study, we were able to observe MST in an SI-5CN, before thermal degradation could occur, by carefully controlling the molecular weight of an SI diblock copolymer. Interestingly, we have observed that during heating a sphere-forming SI-5CN undergoes LDOT and then DMT, transforming into the homogeneous phase, an observation made previously in *neat* SI block diblock copolymers.³² Thus, we conclude that the occurrence of LDOT and DMT in sphere-forming copolymer is not confined to neat SI block copolymer.

We have found that 5CN-COOH synthesized in this study has a T_{cl} of 170 °C. After it is grafted onto the PI block of an SI diblock copolymer, the resulting side-chain LC block copolymer SI-5CN has a T_{cl} of only 84 °C. We have learned from FTIR spectroscopy that such a large difference in T_{cl} between 5CN-COOH and the LC phase of SI-5CN is due to the disappearance of hydrogen bonding present in 5CN-COOH after it is grafted onto the SI block copolymer.

Today it is well established^{36,37} that the molecular weight, block composition, and the degree of segmental interactions between the constituent blocks determine MST or ODT in a block copolymer. When a block copolymer is chemically modified as is in the present study, segmental interactions between the constituent blocks are expected to play a very important role in determining MST or ODT. To investigate the possible role of segmental interactions between the constituent blocks in SI-5CNs, we synthesized two homopolymers, PS-4 and PI-4-5CN. For this, we first hydroxylated a low-molecular-weight PI-4 to obtain PI-4-OH, and then 5CN-COOH was grafted onto PI-4-OH, yielding PI-4-5CN. In the preparation of PI-4-5CN, we varied the amount of 5CN-COOH grafted onto PI-4-OH. We then prepared (PS-4)/(PI-4-5CN) blends to conduct cloud point measurements. We have found that (PS-4)/(PI-4-5CN) blends exhibit an upper critical solution temperature, and the critical temperature is increased as the amount of 5CN-COOH in PI-4-5CN is increased. Thus, we have observed that the segmental interactions between PS-4 and PI-4-5CN become progressively *repulsive* as the amount of 5CN-COOH in PI-4-5CN is increased. Such an observation has led us to conclude that the formation of microdomain structure in SI-5CN is, at least in part, due to an increase in repulsive segmental interactions between the PS and PI-5CN blocks in SI-5CN, compared to the segmental interactions between PS and PI blocks in SI diblock copolymer.

Needless to say, an increase in molecular weight, after 5CN-COOH is grafted onto the PI diblock of SI diblock copolymer, also played an important role in the formation of microdomain structure in SI-5CN.

The side-chain LC block copolymers, SI-5CNs, synthesized in this study have the clearing temperature lower than the MST temperature, i.e., $T_{cl} < T_{MST}$. In principle, the morphology of side-chain LC block copolymer can be manipulated by proper design of the chemical structures of LC monomer and the molecular weight of a block copolymer, such that both microphase-separated structure and the morphology of LC phase, only the morphology of LC phase, or only microphase-separated structure can be observed over a certain range of temperatures. Such an investigation is worth pursuing in the future.

References and Notes

- (1) Fradet, A.; Heitz, W. *Makromol. Chem.* **1987**, *188*, 1613.
- (2) Adams, J.; Gronski, W. *Makromol. Chem., Rapid Commun.* **1989**, *10*, 553.
- (3) Adams, J.; Gronski, W. In *Liquid-Crystalline Polymers*; Weiss, W. A., Ober, C. K., Eds.; ACS Symposium Series No. 435; American Chemical Society: Washington, DC, 1990; p 174.
- (4) Hefft, M.; Springer, J. *Makromol. Chem., Rapid Commun.* **1990**, *11*, 397.
- (5) Sato, M.; Kobayashi, T.; Komatsu, F.; Takeno, N. *Makromol. Chem., Rapid Commun.* **1991**, *12*, 269.
- (6) Wang, J.; Lenz, R. W. *Polym. Eng. Sci.* **1991**, *31*, 739.
- (7) Zaschke, B.; Frank, W.; Fischer, H.; Schmutzler, K.; Arnold, M. *Polym. Bull. (Berlin)* **1991**, *27*, 1.
- (8) Kodaira, T.; Mori, K. *Makromol. Chem.* **1992**, *193*, 1331.
- (9) Percec, V.; Lee, M. *J. Macromol. Sci., Chem.* **1992**, *A29*, 723.
- (10) Komiya, Z.; Schrock, R. R. *Macromolecules* **1993**, *26*, 1387.
- (11) Galli, G.; Chiellini, E.; Yagci, Y.; Serhatli, E. I.; Laus, M.; Bignozzi, M. C.; Angeloni, A. S. *Makromol. Chem., Rapid Commun.* **1993**, *14*, 185.
- (12) Galli, G.; Chiellini, E.; Laus, M.; Angeloni, A. S.; Bignozzi, M. C.; Francescangeli, O. *Mol. Cryst. Liq. Cryst.* **1994**, *254*, 429.
- (13) Fischer, H.; Poser, S.; Arnold, M.; Frank, W. *Macromolecules* **1994**, *27*, 7133.
- (14) Arnold, M.; Poser, S.; Fischer, H.; Frank, W.; Utschick, H. *Macromol. Rapid Commun.* **1994**, *15*, 487.
- (15) Bohnett, R.; Finkelmann, H. *Macromol. Chem. Phys.* **1994**, *195*, 689.
- (16) Yamada, M.; Iguchi, T.; Hirao, A.; Nakahama, S.; Watanabe, J. *Macromolecules* **1995**, *28*, 50.
- (17) Fischer, H.; Poser, S.; Arnold, M. *Macromolecules* **1995**, *28*, 6957.
- (18) Zheng, W. Y.; Hammond, P. T. *Macromol. Rapid Commun.* **1996**, *17*, 813.
- (19) Wang, J.; Mao, G.; Ober, C. K.; Kramer, E. J. *Macromolecules* **1997**, *30*, 1906.
- (20) Mao, G.; Wang, J.; Clingman, S. R.; Ober, C. K.; Chen, I. J.; Thomas, E. L. *Macromolecules* **1997**, *30*, 2556.
- (21) Sanger, J.; Gronski, W.; Maas, S.; Stuhn, B.; Heck, B. *Macromolecules* **1997**, *30*, 6783.
- (22) Zheng, W. Y.; Hammond, P. T. *Macromolecules* **1998**, *31*, 711.
- (23) (a) Yamada, M.; Iguchi, T.; Hirao, A.; Nakahama, S.; Watanabe, J. *Polym. J.* **1998**, *30*, 23. (b) Yamada, M.; Itoh, T.; Nakagawa, R.; Hirao, A.; Nakahama, S.; Watanabe, J. *Macromolecules* **1999**, *32*, 282.
- (24) Sentenac, D.; Demirel, A. L.; Lub, J.; de Jeu, W. H. *Macromolecules* **1999**, *32*, 3235.
- (25) Anthamatten, M.; Zheng, W. T.; Hammond, P. T. *Macromolecules* **1999**, *32*, 4838.
- (26) Anthamatten, M.; Hammond, P. T. *Macromolecules* **1999**, *32*, 8066.
- (27) Lee, K. M.; Han, C. D. *Macromolecules* **2002**, *35*, 760.

- (28) Kim, S. S.; Han, C. D. *Macromolecules* **1993**, *26*, 3176.
- (29) Neumann, C.; Loveday, D. R.; Abetz, V.; Stadler, R. *Macromolecules* **1998**, *31*, 2493.
- (30) (a) Han, C. D.; Kim, J. *J. Polym. Sci., Polym. Phys. Ed.* **1987**, *25*, 1741. (b) Han, C. D.; Kim, J.; Kim, J. K. *Macromolecules* **1989**, *22*, 383. (c) Han, C. D.; Baek, D. M.; Kim, J. K. *Macromolecules* **1990**, *23*, 561.
- (31) (a) Gouinlock, E. V.; Porter, R. S. *Polym. Eng. Sci.* **1977**, *17*, 535. (b) Chung, C. I.; Lin, M. I. *J. Polym. Sci., Polym. Phys. Ed.* **1978**, *16*, 545. (c) Widmaier, J. M.; Meyer, G. C. *J. Polym. Sci., Polym. Phys. Ed.* **1980**, *18*, 2217.
- (32) (a) Han, C. D.; Vaidya, N. T.; Kim, D.; Shin, G.; Yamaguchi, D.; Hashimoto, T. *Macromolecules* **2000**, *33*, 3767. (b) Sakamoto, N.; Hashimoto, T.; Han, C. D.; Kim, D.; Vaidya, N. Y. *Macromolecules* **1997**, *30*, 1621. (c) Sakamoto, N.; Hashimoto, T.; Han, C. D.; Kim, D.; Vaidya, N. Y. *Macromolecules* **1997**, *30*, 5311.
- (33) Dormidontova, E. E.; Lodge, T. P. *Macromolecules* **2001**, *34*, 9143.
- (34) Semenov, A. N. *Sov. Phys. JETP* **1985**, *61*, 733.
- (35) Semenov, A. N. *Macromolecules* **1989**, *22*, 2849.
- (36) Helfand, E.; Wasserman, A. R. *Macromolecules* **1976**, *9*, 879; **1978**, *11*, 960; **1980**, *13*, 994.
- (37) Leibler, L. *Macromolecules* **1980**, *13*, 1602.
- (38) Matsen, M. W.; Bates, F. S. *Macromolecules* **1996**, *29*, 1091.
- (39) Matsen, M. W.; Bates, F. S. *J. Chem. Phys.* **1997**, *106*, 2436.
- (40) Han, C. D. *Multiphase Flow in Polymer Processing*; Academic Press: New York, 1981; Chapter 3.
- (41) Han, J. H.; Fan, D.; Choi-Feng, C.; Han, C. D. *Polymer* **1975**, *36*, 155 and references therein.
- (42) (a) Yoon, P. J. Effect of Thermal History on the Rheology of Thermoplastic Polyurethanes. Doctoral Dissertation, University of Akron, Akron, OH, 1999. (b) Yoon, P. J.; Han, C. D. *Macromolecules* **2000**, *33*, 2171.
- (43) A Gnomix PVT apparatus was used to obtain an expression for the temperature dependence of specific volume for PI-5CN. The experimental procedures employed are as follows. The cell was filled with 1 g of polymer sample and 90 g of mercury; the apparatus was calibrated at 30 °C and 1 atm. Then the sample was pressurized to 10 MPa for the first run. The temperature was controlled to within ± 0.1 °C, and at least 1 h after 20 °C jump was allowed for the sample to equilibrate. At a predetermined temperature data were collected at pressures of 10, 15, 20, 25, 30, 35, 40, 45, 50, 60, 70, 80, 90, and 100 MPa. For each pressure chosen, the sample is held for 40 s before data are taken. The PVT apparatus measures the volume changes in a sample between the measurement condition (temperature T and pressure P) and the reference condition (reference temperature T_r of 30 °C and reference pressure P_r of 10 MPa). The actual volume of the sample at the measurement temperature and pressure, \bar{V}_T^P , was obtained by adding the volume at the reference temperature and pressure, $\bar{V}_{30^\circ\text{C}}^{10\text{MPa}}$, to the volume change recorded during experiment, $\Delta\bar{V}_T^P$. The temperature dependence of specific volume above the clearing temperature of PI-5CN was curve-fitted to a linear relationship, $v = 1.2805 + 3.68 \times 10^{-4} (T - 273)$ (cm³/g).
- (44) Richardson, M. J.; Savill, N. G. *Polymer* **1977**, *18*, 3.

MA012036X